A Revision of CIECAM97s for Practical Applications

Mark D. Fairchild
Munsell Color Science Laboratory
Chester F. Carlson Center for Imaging Science
Rochester Institute of Technology
54 Lomb Memorial Drive
Rochester, New York 14623-5604 USA
mdf@cis.rit.edu

Abstract: The CIE 1997 Interim Color Appearance Model (Simple Version), abbreviated CIECAM97s, was proposed by CIE TC1-34 in 1997 in response to the needs of the imaging industry for a single, practically-applicable, color appearance model for device-independent color imaging applications. CIECAM97s has been successful in focusing a large number of researchers in a single direction to implement, evaluate, and suggest improvements for a single, CIE model. However, CIECAM97s has been less successful in achieving the goal of being practically applicable. CIECAM97s remains a complex color appearance model and this complexity seems to be somewhat of a barrier for its widespread adoption and use. CIE TC8-01 is currently working toward recommendations for practical application of CIECAM97s. Part of TC8-01's work is the consideration and evaluation of potential revisions and simplifications of CIECAM97s. This paper incorporates several previously proposed enhancements of CIECAM97s and a few new suggestions into a revised model for the consideration of TC8-01. It is hoped that this revision will aid in focussing ongoing model tests and perhaps be the starting point for a new CIE recommendation once sufficient testing and perhaps further refinements are completed.

Keywords: Color Appearance Models, CIECAM97s, Color Imaging

INTRODUCTION

In March 1996 the CIE held an expert symposium on *Colour Standards for Image Technology* in Vienna.[1] The symposium covered many image technology concepts for which the CIE might provide guidance or standards to assist industry and ultimately resulted in the formation of CIE Division 8, *Image Technology*. One critical issue raised at the symposium was the establishment of a general-use color appearance model. Symposium participants recognized the need for a color appearance model and requested CIE guidance in establishing a single model that could be used in imaging applications. The task of establishing this model was assigned to CIE TC1-34 and the result of their work was the establishment of the CIE 1997 Interim Color Appearance Model (Simple Version), CIECAM97s, one year later.[2] CIECAM97s has been successful in focusing researchers and practitioners in color science and color imaging on a single color appearance model. This focus has resulted in a number of publications and conference presentations detailing the performance of CIECAM97s and suggestions for improvement. However, CIECAM97s is still not ubiquitous in terms of practical applications. One possible reason for this is the complexity of the model. Despite the intention of TC1-34 that CIECAM97s be a simple model for practical applications, it retains significant complexity and is not easily inverted. The complexity of the model makes it troublesome to implement uniformly in practice and the difficulty in accurately inverting the model limits its practicality in image reproduction applications. Recognizing these difficulties with CIECAM97s, the CIE has created TC8-01, *Colour Appearance Modeling for Colour Management Applications*, to make recommendations on usage, implementation, and possible revision of CIECAM97s. The objective of this paper is to contribute to the ongoing work of TC8-01 by collecting a number of suggested improvements to CIECAM97s along with some newly proposed revisions into a single overall revised model. It is hoped that this revision will serve as a starting point for further investigations within TC8-01 and by others interested in the practical application of color appearance models. Eventually, TC8-01 might recommend a revised version of CIECAM97s for adoption by the

CIE. The revisions described in this paper should serve as a good draft model for this endeavor, if not the final recommendation.

PROPOSED REVISIONS

Essentially as soon as CIECAM97s was established, investigators began to suggest ways it might be improved or simplified. For example, Moroney[3] quickly pointed out some anomalies in the treatment of surround and the lightness scales that were immediately discussed and resolved by members of TC8-01 and Fairchild[4] suggested some ways that the model could be simplified. The following objectives were established for this proposed revision of CIECAM97s:

1. Linearize the chromatic adaptation transform to simplify the model and facilitate inversion,[5-8]
2. Fix the anomalous surround compensation,[3,9,10]
3. Fix the lightness scale for perfect black stimuli,[3,9,10]
4. Fix chroma-scale expansion for colors of low chroma,[11,12] and
5. Make the surround compensation continuously variable.[13,14]

Details and motivations for each of the above revisions are described in the following paragraphs. Other features of the model that might be considered for revision are a reformulation of the degree of adaptation factor, inclusion of mechanisms for black-point adaptation, and general simplification of the model structure. Concepts for treatment of these features are also discussed below.

Linearized Chromatic Adaptation Transform

Two features of the chromatic adaptation transform incorporated into CIECAM97s make it unique. One is the transformation to spectrally-sharpened RGB responses and the second is the adaptation-level-dependent exponential nonlinearity on the B channel. It is this nonlinearity that forces the normalization of tristimulus values to the Y value of the stimulus and renders CIECAM97s uninvertable. It was established by TC1-34 that the CIECAM97s adaptation transform performed as well as, or better than, other proposed models. Thus TC1-34 decided that it's added complexity was worth the improved performance. It is natural to question the importance of each of these two unique features in enabling the performance of CIECAM97s. This was done in the work of TC1-34 in which it was determined that the unique RGB transform was required for good performance since substitution with typical cone responses degraded the model. TC1-34 also determined that the nonlinearity of the B response was required. However, a systematic investigation of the combination of the RGB transform and the nonlinearity was not completed by TC1-34. More recently, the question of whether a similarly-performing model could be formulated by removing the B-channel nonlinearity and optimizing the RGB transform. Results presented by Finlayson and Süsstrunk[5,6] and Li *et al*.[7,8] and further analyses completed in the preparation of this paper all suggest that it is possible to create a linear, von Kries-type adaptation transform that performs as well as, if not better than, the nonlinear transform in CIECAM97s.

Finlayson and Süsstrunk[5,6] demonstrated that direct optimization of a von Kries-type adaptation transformation could lead to a linear model with an optimal RGB transformation that performed at least as well as the CIECAM97s transformation for a collection of corresponding-colors data. Their work is ongoing and has been recently summarized in a paper by Süsstrunk *et al.*[15] that includes a recommended XYZ-to-RGB transformation for a linear adaptation model based on a spectral sharpening optimization. Li *et al.*[7,8] have proposed a revision of the adaptation model in CIECAM97s that includes an optimized XYZ-to-RGB transformation and elimination of the B-channel nonlinearity in addition to a few other modifications. Their optimization was also performed on corresponding-colors data, but by iteratively minimizing the CIELAB color difference between the predicted and observed results. They have also provided[16] a slightly modified version of this transformation by repeating their optimization on a subset of the corresponding colors data (excluding data obtained from a successive-haploscopic experiment with deficient adaptation levels). Finally, a fourth optimization was completed in the process of formulating the revised CIECAM97s model presented in this paper. This optimization was performed using the real samples from the *Munsell Book of Color* (not the extrapolated notations).[11] Using these samples, corresponding colors for a change in adaptation from CIE Illuminant D65 to CIE Illuminant A were calculated using the adaptation transform incorporated in CIECAM97s. This combination was selected since it is an extreme exercise of the adaptation transform and also one for which the CIECAM97s model exhibited superior performance. These corresponding-colors data were used to build a linear von Kries-type adaptation transformation in which the XYZ-to-RGB transformation was optimized in order to minimize CIELAB color differences between the CIECAM97s predictions and the new model predictions. Thus, the objective was to derive a linear model that performed most like the current model incorporated in CIECAM97s.

It is encouraging that three separate studies, completed in three separate laboratories, have reached the same conclusion that an optimized linear chromatic adaptation transform can be substituted for the nonlinear transform in CIECAM97s. Each of the three studies produced models with similar performance and slightly different matrix transformations from XYZ to RGB. It is probably safe to assume that any of the four transforms could be used without changing the real performance of a revised color appearance model significantly. Therefore, it seems clear that a switch to a linear adaptation transform is both acceptable and desirable. The only remaining question is a decision on just which transformation to recommend. Since the performance of all four models is not significantly different when examining visual data, another criterion must be established to make a decision. It is recommended that the best choice is a revised model that produces results as similar as possible to the current CIECAM97s model. The four alternatives were evaluated with respect to the D65-to-A corresponding colors data for the Munsell samples. The Li *et al.*[7,8] matrix produces an average CIELAB color difference from the CIECAM97s model of 2.97. Interestingly this is almost identical to the mean difference of 2.99 reported by Li *et al.*[8] for a large collection of visual corresponding colors data. The modified Li *et al.*[16] matrix produces a mean ΔE^*_{ab} of 1.69. This is significantly more similar to the original CIECAM97s transform since questionable corresponding-colors data were eliminated from the optimization. The spectrally-sharpened matrix from the Süsstrunk *et al.* work[6,16] performed more closely to CIECAM97s, producing a mean ΔE^*_{ab} of 1.51. Lastly, as would be expected, the optimized model produced the lowest mean ΔE^*_{ab} of 0.76. Thus, the Süsstrunk *et al.* model is about a factor of 2 closer to CIECAM97s than the Li *et al.* model and the optimized model is yet another factor of 2 closer. It is clear that TC8-01 should seriously consider a linear adaptation model in any proposed revision of CIECAM97s. The exact choice of the XYZ-to-RGB transform matrix is subject to some interpretation from the three studies described above. However, it appears that any of the four would be adequate. Given this, the optimized matrix producing the smallest change from the current CIECAM97s formulation is recommended and included in Eq. 2. For potential future comparisons of the various proposed matrices, they are all included in Appendix C. Figure 1 shows the RGB responsivities obtained using the transform in Eq. 2 applied to the CIE 1931 Standard Colorimetric Observer. These functions are quite similar to those in CIECAM97s and the modified functions of Li *et al.*[8] One significant difference is that the functions in Fig. 1 show slightly more negative R response in the short-wavelength region of the spectrum. The transform in Eq. 2 (responsivities in Fig. 1) is quite similar to the spectrally sharpened transform of Süsstrunk *et al.*[16] It can be considered a sharpened transform since the responsivities are narrower than typical cone responsivities. They are not, however, optimally sharpened sensors in the sense described by Süsstrunk *et al.*[16] Comparison of the matrices themselves (see App. C) also illustrates the similarity of the transforms; only the R responses significantly differ.

It is reasonable to question the necessity for using sharpened responsivities for the chromatic adaptation transform in CIECAM97s and then converting to the Hunt-Pointer-Estevez cone responsivities to construct the CIECAM97s color space. Why can't the Hunt-Pointer-Estevez responsivities be used for the adaptation transform? Why can't the sharpened transform be used for the color space? TC1-34 did examine these various combinations when formulating CIECAM97s and concluded that an accurate color space could not be easily constructed with the sharpened responses and an accurate adaptation transform could not be easily constructed using cone responsivities. For example, a linear von Kries adaptation transform using the Hunt-Pointer-

Eztevez cone responsivities was compared with the CIECAM97s adaptation transform as described above for the other candidate transforms. This resulted in an average ΔE^*_{ab} of 4.02, clearly significantly different from the CIECAM97s transform that has been shown to be among the best available. The physiological interpretation of this result is that either the von Kries transformation is too simple to describe what actually happens in the visual system, or the visual system applies a von Kries-type transformation to a combination of the cone signals rather than individual cone signals. The most plausible explanation is that the many physiological mechanisms of chromatic adaptation (sensory and cognitive) result in color appearances that tend toward an approximation of the concept of color constancy. It is easily shown mathematically that a von Kries transform predicts more accurate color constancy as the responsivities used are narrowed. In the extreme of monochromatic responsivities, color constancy is perfect with a von Kries transformation.

Anomalous Surround Compensation

As pointed out by Moroney,[3] discussed within TC8-01, and then published in a revision by Li *et al.*,[9,10] the original formulation of CIECAM97s produced non-monotonic changes in appearance with changes in surround relative luminance. This was attributed to the N_c paramaters of 1.0, 1.1, and 0.8 for average, dim, and dark surrounds respectively. Li *et al.*[9,10] suggest using a value of 0.95 for N_c with dim surrounds to produce the expected monotonic behavior. This revision has been widely accepted and is included in table I.

Lightness Scale for Black Stimuli

Similarly, Moroney[3] illustrated that the CIECAM97s lightness values, J, for perfect black stimuli with Y = 0 were not always zero. This effect is certainly possible in a strict visual sense, however it provides difficulties in image reproduction applications in which it is useful to have a more stable black point. This is also congruous with the performance of CIELAB L*, which is widely used in imaging applications. Again, TC8-01 developed a solution by modifying the formula for the achromatic response, A, to subtract 3.05 (all of the noise introduced in the adapted cone signals) rather than 2.05 (which leaves an additive noise of 1.0) thus assuring that stimuli with Y = 0 would always produce no achromatic response. This reformulation was also adopted in the revised model of Li *et al.*[9,10] and is incorporated in Eq. 22 of the current revision.

Chroma-Scale Expansion

Moroney[3] showed how the CIECAM97s chroma scale is expanded at low chroma levels in comparison with CIELAB chroma, C*. This was further illustrated by Wyble *et al.*[11] using the Munsell chroma scales. Wyble *et al.*[11] showed that models fitted to the LUTCHI color appearance data,[17] such as CIECAM97s, showed this systematic expansion of low chroma values. Newman *et al.*[12] showed that this expansion of low chroma could produce detrimental effects in image reproduction applications that require gamut mapping.

It is hypothesized that the LUTCHI experiments might have resulted in expanded scales for chroma (actually colorfulness was scaled) of near neutrals since the scaling was performed with simple patches on uniform achromatic backgrounds. Thus a chromatic crispening effect might well have expanded the chroma scale for near neutrals. On the other hand, Munsell chroma scales were visually scaled as a full global scale (several samples at a time rather than just one) and therefore might better reflect the perception of chroma in complex scenes. Thus an appearance model with a chroma scale more closely approximating the Munsell chroma scale might perform better in imaging applications and avoid the surprising results reported by Newman *et al.*[12]

Further analysis of the Wyble *et al.*[11] results suggested a revision in the CIECAM97s chroma formula to resolve this difficulty. A simple power function was derived to adjust the CIECAM97s chroma function to make the best possible linear prediction of the Munsell chroma scales. This optimized chroma scale is related to the original CIECAM97s chroma scale by raising the original chroma scale to a power of 1.41 and multiplying by 0.2129. This transformation was performed on the original CIECAM97s chroma equation to produce the revised chroma formula in Eq. 26. The relationship between CIECAM97s chroma, and the revised chroma scale is shown in Fig. 2.

Continuous Surround Compensation

The effect of surround on image contrast is well known, but it is also not well understood or quantified.[13] Generally, as in CIECAM97s, surround is treated as a categorical variable with parameters defined for average, dim, and dark surrounds. It is becoming clear that the precise influence of surround is very dependent on the particular viewing conditions and observational task.[14,18] Thus it becomes advantageous to provide an easy way to allow intermediate surround compensations to be performed within a color appearance model[14] (and TC8-01 agreed that such a capability should be incorporated in proposed revisions to CIECAM97s at its April, 2000 meeting). For example, in some models the surround compensation is controlled by a single exponent that can be varied continuously depending on the application. In CIECAM97s, the surround compensation is controlled by two parameters, c and N_c, that are selected based on the average, dim, or dark surround categories. Thus it is important to make sure that both are varied in a consistent manner if intermediate values are to be used. Given the paucity of experimental data available to guide the selection of surround parameters, it is proposed that the c parameter be used as a continuous variable if desired and that the N_c parameter be selected as a function of the c parameter as illustrated in Fig. 3. The function in Fig. 3 is defined as a two-segment piece-wise linear function with the three control points defined by the revised CIECAM97s parameter settings in table I. Thus, when using intermediate (or more extreme) values of c in the revised CIECAM97s calculations, the appropriate value of N_c is obtained via linear interpolation (or extrapolation).

Degree-of-Adaptation Factor

Li *et al.*[7,8] have proposed two new formulas for the computation of the degree of adaptation factor, D. Their formulas are similar in concept to the formula incorporated in CIECAM97s, but differ in structure. Since these formulas are in a state of flux and it is unclear that the revisions are warranted by the available data, the revised model presented in this paper retains the CIECAM97s D formula as given in Eq. 6. Another reason for retaining the CIECAM97s D formula is that the D factor has come to be used in imaging applications to optimize for specific applications[19] and users might be accustomed to the current formulation. Clearly the use and formulation of the D factor is an important part of any revision to CIECAM97s and if new methods to derive or utilize the D factor can be formulated, they should be considered for inclusion in a revised model. At this time there appears to be no justification for changing Eq. 6.

Black-Point Adaptation

It is conceivable that the human visual system is capable of adapting to the black point, as well as the white point, of a scene or stimulus configuration. In essence, this can be thought of as an automated mechanism to adapt to scenes of various dynamic ranges such that the minimum luminance is perceived as black and the maximum as white. There is currently no capability within CIECAM97s to model such adaptation (although the modification of the achromatic response to assure that $J = 0$ for $Y = 0$ is a step in that direction). While black-point adaptation is becoming a topic of significant interest for image reproduction, appearance modeling, and gamut mapping, there is currently no universally accepted visual model for this phenomenon (if it even exists). Thus it is premature to recommend a revision to CIECAM97s for black-point adaptation. In the interim, if it becomes necessary to somehow model black point adaptation, a possible technique is to subtract the tristimulus values of the black point from each stimulus tristiumulus value such that the minimum values are zero. The tristimulus values can then be multiplicatively scaled such that a perfect white (or other reference white) has a Y tristimulus value of 100. Thus, black-point adaptation could be considered as a preprocessing strategy prior to the color appearance calculations. This can be thought of as similar to the use of normalized tristimulus values (normalized to the device gamut) commonly found in imaging applications. Note that such a transformation will impact the predicted appearance of all colors in an image (generally increasing the predicted chroma). Other possible techniques might involve transformation of the black point in the CEICAM97s appearance space (*e.g.*, mapping the lightness, J). Such techniques begin to cross over the line between color appearance modeling and gamut mapping algorithms.

General Simplification

Fairchild[4] has shown how the general structure of CIECAM97s could be modified to produce a significantly simpler model. Beyond a simplification of table I that eliminates the need for the F_{LL} parameter, no such simplifications or structural refinements were incorporated in the current revision. While there is certainly simplicity to be gained without the loss of model performance, this would require a restructuring of the model that would essentially constitute formulation of a new model. Since CIECAM97s is being used and tested on a scope that might be quite extensive, there is an important efficiency of effort that is obtained by minimizing the number and extent of proposed revisions. Thus, the structure of CIECAM97s was retained to the extent possible while incorporating the five major revisions listed above that have apparently reached some level of consensus with respect to their need.

Terminology

Color appearance models aim to provide mathematical relationships between physically measurable properties of stimuli (*e.g.*, CIE tristimulus values) and the appearance attributes of visual sensations (*e.g.*, lightness, brightness, chroma, hue, colorfulness, and saturation). It is important that the definitions of these terms and there appearance model correlates be used consistently. All terms in this paper and in the CIE reports on CIECAM97s follow the definitions of the *International Lighting Vocabulary*.[20] Their typical usage in the colour appearance field is also further discussed in Fairchild.[21]

THE REVISED CIECAM97s MODEL

The following paragraphs detail the formulation and implementation of the revised CIECAM97s model as described in the previous section. To the extent possible, the revised model follows the original CIECAM97s presentation and implementation.

Input Data

The model input data are the adapting field luminance in cd/m^2 (normally taken to be 20% of the luminance of white in the adapting field), L_A, the relative tristimulus values of the stimulus, XYZ, the relative tristimulus values of white in the same viewing conditions, $X_wY_wZ_w$, and the relative luminance of the background, Y_b. Relative tristimulus values should be expressed on a scale from Y = 0 for a perfect black to Y = 100 for a perfect reflecting diffuser. Additionally, the parameters c, for the impact of surround, N_c, a chromatic induction factor, and F, a factor for degree of adaptation, must be selected according to the guidelines in table I and the further discussion below. Note that the F_{LL} parameter has been removed from CIECAM97s since it only functioned for large stimuli that are not found in imaging applications. All CIE tristimulus values are obtained using the CIE 1931 Standard Colorimetric Observer (2°). Background is defined as the area immediately adjacent to the stimulus of interest and surround is defined as the remainder of the visual field. Surround relative luminances of greater than or approximately equal to 20% of the scene white are considered average, less than 20% are considered dim, and approximately 0% are considered dark.

Table I. Selection guidelines for parameters used in the revised model.

Viewing Condition	c	N_c	F
Average Surround	0.69	1.0	1.0
Dim Surround	0.59	0.95	0.9
Dark Surround	0.525	0.8	0.9

In order to make the surround compensation in CIECAM97s continuously variable, both c and N_c must be varied together. It is proposed that the three points in table I be used to define a two-part piecewise-linear function relating N_c to c as shown in Fig. 3. Thus, a simple linear interpolation as illustrated in Fig. 3 can be used to determine intermediate values of N_c given selected intermediate values of c. Perhaps in time further data will become available to allow a more rigorous continuously-varying definition of c and N_c.

Chromatic Adaptation

An initial chromatic adaptation transform is used to go from the stimulus viewing conditions to corresponding colors under implicit equal-energy-illuminant reference viewing conditions. First, tristimulus values for both the sample and white and transformed to spectrally-sharpened cone responses, illustrated in Fig. 1, using the transformation given in Eqs. 1 and 2. Since the chromatic adaptation transform has been linearized, it is no longer required to divide the stimulus tristimulus values by their own Y tristimulus value prior to the chromatic adaptation transformation.

$$\begin{bmatrix} R \\ G \\ B \end{bmatrix} = \mathbf{M} \begin{bmatrix} X \\ Y \\ Z \end{bmatrix} \tag{1}$$

$$\mathbf{M} = \begin{bmatrix} 0.8562 & 0.3372 & -0.1934 \\ -0.8360 & 1.8327 & 0.0033 \\ 0.0357 & -0.0469 & 1.0112 \end{bmatrix} \qquad \mathbf{M}^{-1} = \begin{bmatrix} 0.9874 & -0.1768 & 0.1894 \\ 0.4504 & 0.4649 & 0.0846 \\ -0.0139 & 0.0278 & 0.9861 \end{bmatrix} \tag{2}$$

The chromatic-adaptation transform is a von Kries-type transformation as given in Eqs. 3 through 5. In addition, the variable D is used to specify the degree of adaptation. D is set to 1.0 for complete adaptation or discounting the illuminant (as is typically the case for reflecting materials). D is set to 0.0 for no adaptation. D takes on intermediate values for various degrees of incomplete chromatic adaptation. Equation 6 allows calculation of such intermediate D values for various luminance levels and surround conditions.

$$R_c = \left[D\left(100/R_w\right) + 1 - D\right]R \tag{3}$$

$$G_c = \left[D\left(100/G_w\right) + 1 - D\right]G \tag{4}$$

$$B_c = \left[D\left(100/B_w\right) + 1 - D\right]B \tag{5}$$

$$D = F - F\Big/\left[1 + 2\left(L_A^{1/4}\right) + \left(L_A^2\right)\Big/300\right] \tag{6}$$

Similar transformations are also made for the white since they are required in later calculations. Various factors must be calculated prior to further calculations as shown in Eqs. 7 through 11. These include a background induction factor, n, the background and chromatic brightness induction factors, N_{bb} and N_{cb}, and the base exponential nonlinearity, z. Only Eq. 11 differs from the CIECAM97s formulation since the F_{LL} factor has been eliminated (effectively always 1.0).

$$k = 1/\left(5L_A + 1\right) \tag{7}$$

$$F_L = 0.2k^4\left(5L_A\right) + 0.1\left(1 - k^4\right)^2\left(5L_A\right)^{1/3} \tag{8}$$

$$n = Y_b / Y_w \tag{9}$$

$$N_{bb} = N_{cb} = 0.725(1/n)^{0.2} \tag{10}$$

$$z = 1 + n^{1/2} \tag{11}$$

The post-adaptation signals for both the sample and the white are then transformed from the sharpened cone responses to the Hunt-Pointer-Estevez cone responses as shown in Eqs. 12 and 13 prior to application of a nonlinear response compression.

$$\begin{bmatrix} R' \\ G' \\ B' \end{bmatrix} = \mathbf{M}_H \mathbf{M}^{-1} \begin{bmatrix} R_c \\ G_c \\ B_c \end{bmatrix} \tag{12}$$

$$\mathbf{M}_H = \begin{bmatrix} 0.38971 & 0.68898 & -0.07868 \\ -0.22981 & 1.18340 & 0.04641 \\ 0.00 & 0.00 & 1.00 \end{bmatrix} \quad \mathbf{M}_H^{-1} = \begin{bmatrix} 1.9102 & -1.1121 & 0.2019 \\ 0.3710 & 0.6291 & 0.00 \\ 0.00 & 0.00 & 1.00 \end{bmatrix} \tag{13}$$

The post-adaptation cone responses (for both the stimulus and the white) are then calculated using Eqs. 14 through 16.

$$R'_a = \frac{40(F_L R'/100)^{0.73}}{\left[(F_L R'/100)^{0.73} + 2\right]} + 1 \tag{14}$$

$$G'_a = \frac{40(F_L G'/100)^{0.73}}{\left[(F_L G'/100)^{0.73} + 2\right]} + 1 \tag{15}$$

$$B'_a = \frac{40(F_L B'/100)^{0.73}}{\left[(F_L B'/100)^{0.73} + 2\right]} + 1 \tag{16}$$

Appearance Correlates

Preliminary red-green and yellow-blue opponent dimensions are calculated using Eqs. 17 and 18.

$$a = R'_a - 12G'_a/11 + B'_a/11 \tag{17}$$

$$b = (1/9)(R'_a + G'_a - 2B'_a) \tag{18}$$

Hue angle, h, is then calculated from a and b using Eq. 19.

$$h = \tan^{-1}(b/a) \tag{19}$$

Hue quadrature, H, and eccentricity factor, e, are calculated from the following unique hue data via linear interpolation between the following values for the unique hues:

Red:	h = 20.14,	e = 0.8,	H = 0 or 400,
Yellow:	h = 90.00,	e = 0.7,	H = 100,
Green:	h = 164.25,	e = 1.0,	H = 200,
Blue:	h = 237.53,	e = 1.2,	H = 300

Equations 20 and 21 illustrate calculation of e and H for arbitrary hue angles where the quantities subscripted 1 and 2 refer to the unique hues with hue angles just below and just above the hue angle of interest.

$$e = e_1 + (e_2 - e_1)(h - h_1)/(h_2 - h_1) \quad (20)$$

$$H = H_1 + \frac{100(h - h_1)/e_1}{(h - h_1)/e_1 + (h_2 - h)/e_2} \quad (21)$$

The achromatic response is calculated as shown in Eq. 22 for both the stimulus and the white. Note that a value of 3.05 is subtracted rather than the 2.05 in the original CIECAM97s formulation.

$$A = \left[2R'_a + G'_a + (1/20)B'_a - 3.05\right]N_{bb} \quad (22)$$

Lightness, J, is calculated from the achromatic signals of the stimulus, A, and white, A_W, using Eq. 23.

$$J = 100(A/A_w)^{cz} \quad (23)$$

Brightness, Q, is calculated from lightness and the achromatic response for the white using Eq. 24.

$$Q = (1.24/c)(J/100)^{0.67}(A_w + 3)^{0.9} \quad (24)$$

Finally, saturation, s; chroma, C; and colorfulness, M; are calculated using Eqs. 25 through 27, respectively. Eq. 26 has been modified to allow accurate prediction of the Munsell chroma scales.

$$s = \frac{50(a^2 + b^2)^{1/2} 100e(10/13)N_c N_{cb}}{R'_a + G'_a + (21/20)B'_a} \quad (25)$$

$$C = 0.7487 s^{0.973} (J/100)^{0.945n} \left(1.64 - 0.29^{n}\right)^{1.41} \tag{26}$$

$$M = C F_L^{0.15} \tag{27}$$

Rectangular Coordinates

CIECAM97s provides mathematical scales to correlate with various perceptual appearance attributes. As such, it does not explicitly construct a color space. The CIECAM97s lightness, chroma, and hue correlates (J,C,h) can be used to construct a color space by considering them as cylindrical coordinates as is done in the CIELAB colour space with L*, C^*_{ab}, and h_{ab}. Alternatively, a brightness-colorfulness space could be constructed using CIECAM97s Q, M, and h as cylindrical coordinates. If rectangular spaces are required, they can be constructed using the normal means for cylindrical-to-rectangular coordinate transformations (*i.e.*, J, Ccos(h), and Csin(h) or Q, Mcos(h), and Msin(h) could be used as rectangular coordinates). Moroney[22] as suggested the following notation for rectangular coordinates based on chroma, colorfulness, and saturation, respectively. This, or similar, notation should be adopted by the CIE for uniform practice.

$$a_C = C\cos(h) \tag{28}$$

$$b_C = C\sin(h) \tag{29}$$

$$a_M = M\cos(h) \tag{30}$$

$$b_M = M\sin(h) \tag{31}$$

$$a_s = s\cos(h) \tag{32}$$

$$b_s = s\sin(h) \tag{33}$$

CONCLUSIONS

CIE TC8-01 is working to establish guidelines for the use of color appearance models in practical imaging applications and investigating possible revisions to the CIECAM97s model. This paper has attempted to compile the most significant and important proposed revisions to CIECAM97s in a single place and thus propose a complete, revised model for the consideration of TC8-01 and further testing and refinement. It is hoped that this compilation will provide the starting point for eventual CIE approval of a revised version of CIECAM97s.

REFERENCES

1. CIE, CIE expert symposium ‘96 Colour standards for image technology. Vienna: CIE Pub. No. x010; 1996.

2. CIE, The CIE 1997 interim colour appearance model (simple version), CIECAM97s. Vienna: CIE Pub. 131; 1998.

3. Moroney N. A comparison of CIELAB and CIECAM97s. Scottsdale: Proceedings of IS&T/SID 6th Color Imaging Conference; 1998. p 17-21.

4. Fairchild MD. The ZLAB color appearance model for practical image reproduction applications. Proceedings of the CIE Expert Symposium '97 on Colour Standards for Image Technology, CIE Pub. x014 1998. p 89-94.

5. Finlayson GD, Drew MS. Positive Bradford curves through sharpening. Scottsdale: Proceedings of IS&T/SID 7th Color Imaging Conference; 1999. p 227-232.

6. Finlayson GD, Süsstrunk S. Performance of a chromatic adaptation transform based on spectral sharpening. Scottsdale: Proceedings of IS&T/SID 8th Color Imaging Conference; 2000. p 49-55.

7. Li C, Luo MR, Rigg B. Simplification of the CMCCAT97. Scottsdale: Proceedings of IS&T/SID 8th Color Imaging Conference; 2000. p 56-60.

8. Li C, Luo MR, Rigg B, Hunt RWG. CMC 2000 Chromatic Adaptation Transform: CMCCAT2000. Color Res Appl 2001; 26:submitted.

9. Li C, Luo MR, Hunt RWG. The CAM97s2 model. Scottsdale: Proceedings of IS&T/SID 7th Color Imaging Conference; 1999. p 262-263.

10. Li CJ, Luo MR, Hunt RWG. A revision of the CIECAM97s model. Color Res Appl 2000; 25:260-266.

11. Wyble DR, Fairchild MD. Prediction of Munsell appearance scales using various color appearance models. Color Res Appl 2000; 25:132-144.

12. Newman T, Pirrotta E. The darker side of colour appearance models and gamut mapping. Derby: Proceedings of Colour Image Science 2000; 2000. p 215-223.

13. Fairchild MD. Considering the surround in device-independent color imaging. Color Res Appl 1995; 20:352-363.

14. Fairchild MD. Refinement of the RLAB color space. Color Res Appl 1996; 21:338-346.

15. Süsstrunk S, Holm, J, Finlayson GD. Chromatic adaptation performance of different RGB sensors. Proceedings of SPIE/IS&T Electronic Imaging 2001; in press.

16. Luo MR. Personal Communication, Nov. 2000.

17. Hunt RWG, Luo MR. Evaluation of a model of colour vision by magnitude scalings: Discussion of collected results. Color Res Appl 1994; 19:27-33.

18. Fairchild MD, Johnson GM. Color appearance reproduction: Visual data and predictive modeling. Color Res Appl 1999; 24:121-131.

19. Henley S, Fairchild MD. Quantifying mixed adaptation in cross-media color reproduction. Scottsdale: Proceedings of IS&T/SID 8th Color Imaging Conference; 2000. p 305-310.

20. CIE. International Lighting Vocabulary. Vienna:CIE Pub. No. 17.4; 1987.

21. Fairchild MD. Color Appearance Models. Reading: Addison-Wesley; 1998.

22. Moroney N. Usage guidelines for CIECAM97s. Portland: Proceedings of IS&T PICS Conference; 2000. p 164-168.

APPENDIX A: NUMERICAL EXAMPLES

Example calculations using the revised model are given for four samples in Table A-I. A Microsoft Excel spreadsheet with these example calculations for this revision of CIECAM97s can be found at <http://www.cis.rit.edu/fairchild/CAM.html>.

Table A-I. Example calculations (with a number of intermediate values) using the revised CIECAM97s model for four samples.

	Case 1	Case 2	Case 3	Case 4
X	19.01	57.06	3.53	19.01
Y	20.00	43.06	6.56	20.00
Z	21.78	31.96	2.14	21.78
X_w	95.05	95.05	109.85	109.85
Y_w	100.00	100.00	100.00	100.00
Z_w	108.88	108.88	35.58	35.58
L_A (cd/m^2)	318.31	31.83	318.31	31.83
F	1.0	1.0	1.0	1.0
D	0.997	0.890	0.997	0.890
Y_b	20.0	20.0	20.0	20.0
c	0.69	0.69	0.69	0.69
N_c	1.0	1.0	1.0	1.0
k	0.001	0.006	0.001	0.006
F_L	1.17	0.54	1.17	0.54
n	0.20	0.20	0.20	0.20
N_{bb}	1.00	1.00	1.00	1.00
N_{cb}	1.00	1.00	1.00	1.00
z	1.45	1.45	1.45	1.45
R	18.81	57.19	4.82	18.81
G	20.83	31.32	9.08	20.83
B	21.76	32.34	1.98	21.76
R_w	94.04	94.04	120.89	120.89
G_w	104.17	104.17	91.55	91.55
B_w	108.80	108.80	35.21	35.21
R_c	20.00	60.42	3.99	15.91
G_c	20.00	30.20	9.91	22.55
B_c	20.01	30.01	5.62	57.43
R_{cw}	99.98	99.35	100.06	102.29
G_{cw}	100.01	100.46	99.98	99.07
B_{cw}	100.03	100.96	99.81	92.90
X_c	20.0	60.0	3.3	22.6
Y_c	20.0	43.8	6.9	22.5
Z_c	20.0	29.6	5.8	57.0
X_{cw}	100.0	99.5	100.0	101.1
Y_{cw}	100.0	100.0	100.0	100.0
Z_{cw}	100.0	101.0	99.8	92.9

R'	20.0	51.2	5.6	19.8
G'	20.0	39.4	7.7	24.1
B'	20.0	29.6	5.8	57.0
R'_w	100.0	99.7	100.0	101.0
G'_w	100.0	100.2	100.0	99.4
B'_w	100.0	101.0	99.8	92.9
R'_a	6.9	7.6	3.5	4.6
G'_a	6.9	6.6	4.2	5.1
B'_a	6.9	5.6	3.6	8.0
R'_{aw}	15.4	10.7	15.4	10.7
G'_{aw}	15.4	10.7	15.4	10.7
B'_{aw}	15.4	10.7	15.3	10.3
a	0.00	0.90	-0.67	-0.22
b	0.00	0.32	0.05	-0.71
h	251.9	19.4	175.3	252.5
H	307.4	399.4	217.6	307.8
H_c (Red)	7	99	0	8
H_c (Yellow)	0	0	0	0
H_c (Green)	0	0	82	0
H_c (Blue)	93	1	18	92
e	1.16	0.80	1.03	1.16
A	17.99	18.94	8.38	11.57
A_w	43.80	29.54	43.80	29.62
J	41.13	64.14	19.18	39.11
Q	31.57	30.66	18.93	22.05
s	0.10	146.59	232.06	183.13
C	0.05	71.22	88.64	80.55
M	0.06	64.97	90.72	73.48
a_C	-0.02	67.19	-88.35	-24.22
b_C	-0.05	23.62	7.20	-76.82
a_M	-0.02	61.29	-90.42	-22.09
b_M	-0.05	21.55	7.36	-70.07
a_s	-0.03	138.30	-231.30	-55.07
b_s	-0.10	48.61	18.84	-174.65

APPENDIX B: Inverting the Revised Model

Steps for using the revised model in the reverse direction for corresponding-colors calculations or color-reproduction applications follow.

Starting Data:

Q or J, M or C, H or h

A_w, n, z, F_L, N_{bb}, N_{cb} Obtained Using Forward Model

Surround Parameters: F, c, N_c

Luminance Level Parameters: L_A, D

Unique Hue Data:

Red: h = 20.14, e = 0.8

Yellow: h = 90.00, e = 0.7

Green: h = 164.25, e = 1.0

Blue: h = 237.53, e = 1.2

(1) From Q Obtain J (if necessary)

$$J = 100(Qc/1.24)^{1/0.67}/(A_w + 3)^{0.9/0.67} \tag{B.1}$$

(2) From J Obtain A

$$A = (J/100)^{1/cz} A_w \tag{B.2}$$

(3) Using H, Determine h_1, h_2, e_1, e_2 (if h is not available)

e_1 and h_1 are the values of e and h for the unique hue having the nearest lower value of h and e_2 and h_2 are the values of e and h for the unique hue having the nearest higher value of h.

(4) Calculate h (if necessary)

$$h = \left[(H - H_1)(h_1/e_1 - h_2/e_2) - 100h_1/e_1\right] / \left[(H - H_1)(1/e_1 - 1/e_2) - 100/e_1\right] \tag{B.3}$$

H_1 is 0, 100, 200, or 300 according to whether red, yellow, green, or blue is the hue having the nearest lower value of h.

(5) Calculate e

$$e = e_1 + (e_2 - e_1)(h - h_1)/(h_2 - h_1) \tag{B.4}$$

e_1 and h_1 are the values of e and h for the unique hue having the nearest lower value of h and e_2 and h_2 are the values of e and h for the unique hue having the nearest higher value of h.

(6) Calculate C (if necessary)

$$C = M / F_L^{0.15} \tag{B.5}$$

(7) Calculate s

$$s = C^{1/0.973} / \left[0.7487(J/100)^{0.945n}(1.64 - 0.29^n)^{1.41}\right]^{1/0.973} \tag{B.6}$$

(8) Calculate a and b

$$a = s(A/N_{bb} + 3.05) / \left\{\left[1 + (\tan h)^2\right]^{1/2}\left[50000 e N_c N_{cb}/13\right] + s\left[(11/23) + (108/23)(\tan h)\right]\right\} \tag{B.7}$$

In calculating $\left[1 + (\tan h)^2\right]^{1/2}$ the result is taken as:

positive for 0° ≤ h < 90°
negative for 90° ≤ h < 270°
positive for 270° ≤ h < 360°.

$$b = a(\tan h) \tag{B.8}$$

(9) Calculate R'_a, G'_a, and B'_a

$$R'_a = (20/61)(A/N_{bb} + 3.05) + (41/61)(11/23)a + (288/61)(1/23)b \tag{B.9}$$

$$G'_a = (20/61)(A/N_{bb} + 3.05) - (81/61)(11/23)a - (261/61)(1/23)b \tag{B.10}$$

$$B'_a = (20/61)(A/N_{bb} + 3.05) - (20/61)(11/23)a - (20/61)(315/23)b \tag{B.11}$$

(10) Calculate R′, G′, and B′

$$R' = \tfrac{100}{F_L}\left[(2R'_a - 2)/(41 - R'_a)\right]^{1/0.73} \tag{B.12}$$

$$G' = \tfrac{100}{F_L}\left[(2G'_a - 2)/(41 - G'_a)\right]^{1/0.73} \tag{B.13}$$

$$B' = \tfrac{100}{F_L}\left[(2B'_a - 2)/(41 - B'_a)\right]^{1/0.73} \quad \text{(B.14)}$$

If R'_a-1 < 0 use:

$$R' = -\tfrac{100}{F_L}\left[(2 - 2R'_a)/(39 + R'_a)\right]^{1/0.73} \quad \text{(B.15)}$$

and similarly for the G′ and B′ equations.

(11) Calculate R_c, G_c, and B_c

$$\begin{vmatrix} R_c \\ G_c \\ B_c \end{vmatrix} = \mathbf{M}\ \mathbf{M}_H^{-1} \begin{vmatrix} R' \\ G' \\ B' \end{vmatrix} \quad \text{(B.16)}$$

(12) Calculate R, G, and B

$$R = R_c / \left[D(100/R_w) + 1 - D\right] \quad \text{(B.17)}$$

$$G = G_c / \left[D(100/G_w) + 1 - D\right] \quad \text{(B.18)}$$

$$B = B_c / \left[D(100/B_w) + 1 - D\right] \quad \text{(B.19)}$$

(15) Calculate X, Y, and Z

$$\begin{vmatrix} X \\ Y \\ Z \end{vmatrix} = \mathbf{M}^{-1} \begin{vmatrix} R \\ G \\ B \end{vmatrix} \quad \text{(B.20)}$$

APPENDIX C: Transformation Matrices

Several XYZ-to-RGB transformation matrices for the chromatic adaptation transform are described in the text. Each of the matrices is given below for reference and potential testing. While it seems quite likely that CIE TC8-01 will adopt a linear chromatic adaptation transform for a revision of CIECAM97s, it remains uncertain just which transformation will be selected.

The optimized transform recommended in this paper and designed to perform most like the original CIECAM97s adaptation transform is given in Eq. 2 in the text and Eq. C.1 below.

$$\mathbf{M} = \begin{bmatrix} 0.8562 & 0.3372 & -0.1934 \\ -0.8360 & 1.8327 & 0.0033 \\ 0.0357 & -0.0469 & 1.0112 \end{bmatrix} \tag{C.1}$$

The Li *et al.*[7] matrix is given in Eq. C.2.

$$\mathbf{M}_{Li} = \begin{bmatrix} 0.7982 & 0.3389 & -0.1371 \\ -0.5918 & 1.5512 & 0.0357 \\ 0.0008 & 0.0239 & 0.9753 \end{bmatrix} \tag{C.2}$$

The modified Li *et al.* Matrix[16] (optimized to a data set excluding some of the disparate haploscopic data) is given in Eq. C.3.

$$\mathbf{M}_{Li2} = \begin{bmatrix} 0.7328 & 0.4296 & -0.1624 \\ -0.7036 & 1.6974 & 0.0061 \\ 0.0030 & 0.0136 & 0.9834 \end{bmatrix} \tag{C.3}$$

The Süsstrunk *et al.*[15] optimized spectrally sharpened matrix is given in Eq. C.4.

$$\mathbf{M}_{Susstrunk} = \begin{bmatrix} 1.2694 & -0.0988 & -0.1706 \\ -0.8364 & 1.8006 & 0.0357 \\ 0.0294 & -0.0315 & 1.0018 \end{bmatrix} \tag{C.4}$$

The Hunt-Pointer-Estevez matrix for normal cone responsivities is given in Eq. 13 in the text and Eq. C.5 below.

$$\mathbf{M}_H = \begin{bmatrix} 0.38971 & 0.68898 & -0.07868 \\ -0.22981 & 1.18340 & 0.04641 \\ 0.00 & 0.00 & 1.00 \end{bmatrix} \tag{C.5}$$

Figure Captions

Figure 1. The "sharpened-cone" responses obtained using the revised transformation matrix, **M**, given in Eq. 2.

Figure 2. The relationship between the original CIECAM97s chroma scale, C, and the revised chroma scale given in Eq. 26.

Figure 3. Piecewise linear function relating the surround parameters c and N_c such that the surround compensation can be implemented in a continuously variable manner.

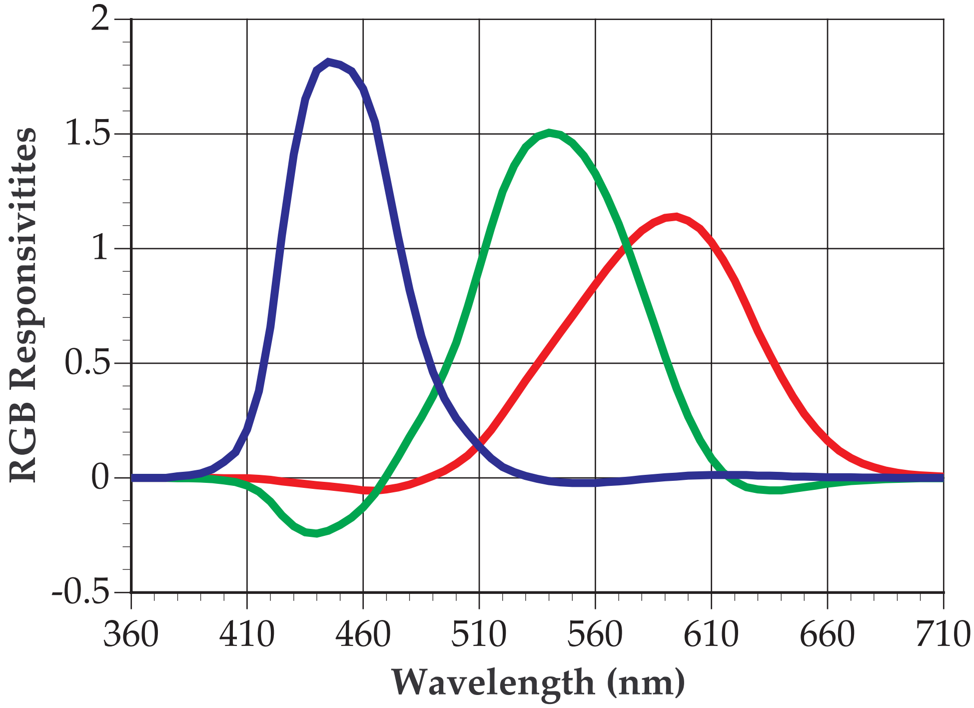
2
1.5
1
0.5
0
-0.5
RGB Responsivitites
360
410
460
510
560
610
660
710
Wavelength (nm)

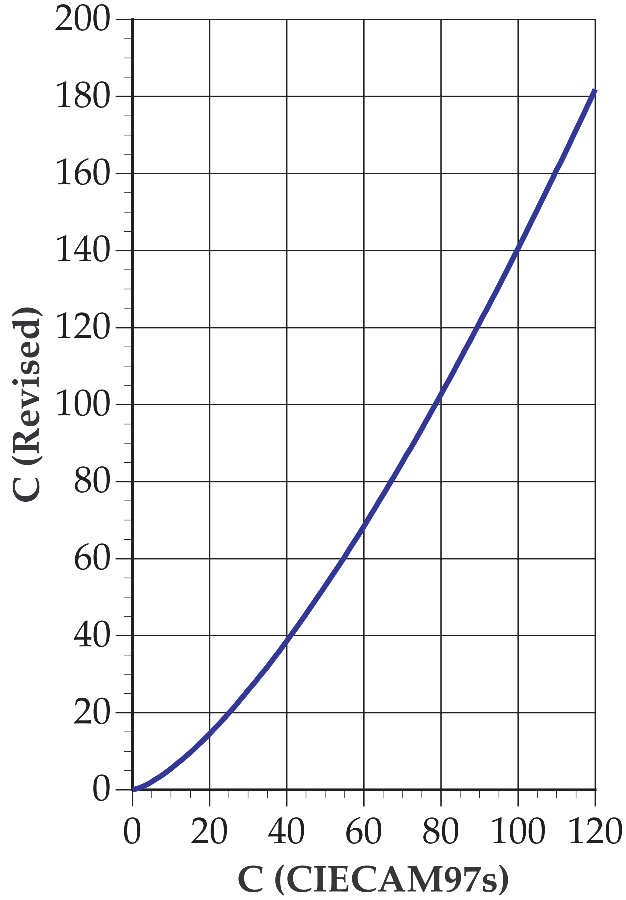
200
180
160
140
120
100
80
60
40
20
0
C (Revised)
0
20
40
60
80
100
120
C (CIECAM97s)

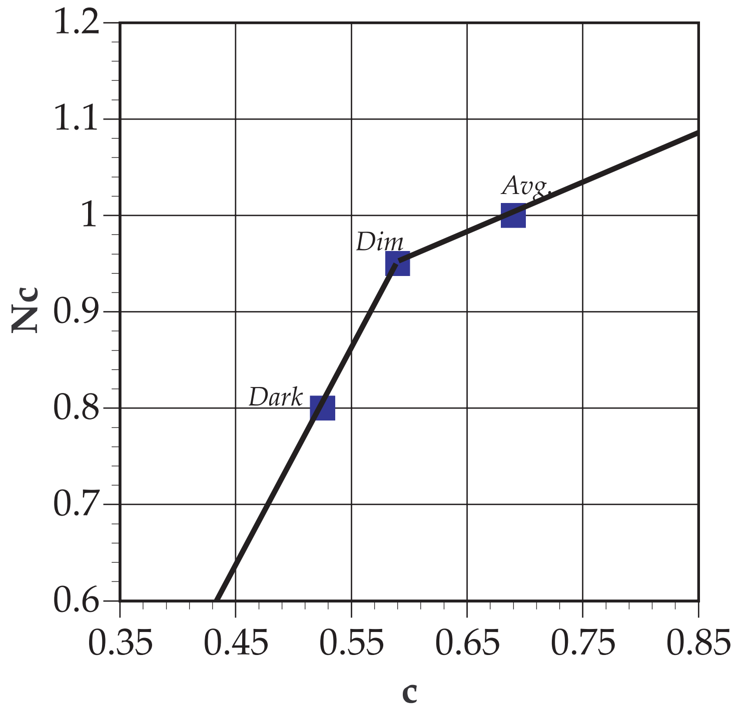

1.2
1.1
1
0.9
0.8
0.7
0.6
Nc
Avg.
Dim
Dark
0.35
0.45
0.55
0.65
0.75
0.85
c